Seismological detection of a mantle plume?

Henri-Claude Nataf & John VanDecar

Department of Theoretical Geophysics, University of Utrecht, PO Box 80021, 3508 TA Utrecht, The Netherlands

A detailed seismological study of the mantle beneath the Bowie hotspot, west of Canada, reveals a zone of low seismic velocities. The anomaly, probed at a depth of ~700 km, adds a delay of 0.15 s to the travel times of seismic waves traversing a region ~150 km in diameter, located ~150 km away from the vertical projection of the Bowie seamount. This observation suggests that a mantle plume is present in the lower mantle beneath Bowie, with the amplitude of the anomaly implying a temperature contrast of about ~300 K.

OVER twenty years ago, Morgan[1] proposed that mantle plumes (diapirs), rising from the core–mantle boundary, were responsible for 'hotspot' volcanoes. These volcanoes are seen to form linear chains on the ocean floor, in the middle of tectonic plates[2], with the most striking example being Hawaii. No better explanation has been proposed since, but several questions remain. Do plumes originate at the core–mantle boundary, or in some hypothetical thermal boundary layer above the 660 km seismic discontinuity[3], or at still shallower[4] depths? Do diapirs rise almost vertically, as the fixity of hotspots with respect to each other suggests, or are they advected by a large convection flow? Is the temperature in the plume 200 K higher than average[5,6] or 800 K higher[7]? How wide are the plumes, and what initiates them?

Much could be learned if seismological data were to bring insights into the deep structure of plumes. A detailed investigation of the Yellowstone hotspot has revealed low seismic velocities (presumably due to high temperatures) in the lithosphere, down to at least 250 km depth (ref. 8) and possibly 400 km (ref. 9). More recently, evidence for slow hotspot material beneath the lithosphere has emerged from high-resolution global tomography[10]. This is consistent with the idea that hot material rising in the plume spreads into a cushion more than 500 km in diameter when impinging on the base of the lithosphere.

What signal is expected at depth?

At greater depths the plume is expected to be only ~100 km in diameter[5–7]. Such a narrow feature would be very difficult to detect. An early indication of a localized slow anomaly at the core–mantle boundary beneath Hawaii[12] was soon discounted as an artefact[13]. Despite the great improvement in regional tomography over the past 10 years[14–16], plumes are yet to be detected by seismologists. Hopes are faint, as both the amplitude of the signal and the width over which it occurs are expected to be very small. A lower bound can be constructed on the basis of temperature and diameter derived from petrology and isotope geochemistry[5,6], and heat balance[17,18]. Typical values are a temperature contrast of 200 K and a diameter of 100 km. Assuming that P-wave velocity varies with temperature as $(1/V)\,dV/dT = -5\times10^{-5}\ K^{-1}$ (ref. 19), one predicts an integrated maximum travel-time delay of 0.1 s. To give an idea of how small this is, arrival times reported to the International Seismological Centre (ISC) are rounded to the nearest 0.1 s. This is, however, a lower bound, as the temperature is based on sub-lithospheric processes, and the temperature contrast is expected to increase as one goes deeper into the mantle. The diameter is also likely to increase with depth, owing to the higher viscosity of the deeper mantle. 'Realistic' mantle convection models[20] produce diapirs with temperature contrasts of ~400 K, and diameters of ~250 km, in the upper mantle. This would produce an integrated maximum travel-time delay of 0.5 s.

The delays computed above are simple integrations of velocity anomalies deduced from simple velocity–temperature relationships, and there are several effects that could increase or decrease the P-wave delays: for example, partial melting and anisotropy due to crystallographic alignment in a vertical flow could increase the time delay. Conversely, it has been thought that the time delay could be severely reduced by 'wavefront healing', a frequency-dependent wave propagation phenomenon[21]; rays diffracted around the edges of the slow region can arrive before, and obliterate, the Fermat ray, thereby reducing the inferred time delay. However, for the small velocity perturbations and smooth variations expected for plumes, we find this effect to be small. Figure 1 shows synthetic seismograms computed for a plane wave travelling through a uniform region containing a plume-like cylindrical anomaly. Two-dimensional synthetic seismograms are constructed using a parabolic approximation to the full wave equation[22]. In the propagation plane, the plume-like anomaly is modelled as a gaussian velocity perturbation with a peak value of −2%, and a diameter of 150 km at $1/e$, centred at the origin (0, 0). The wave accumulates a delay of ~0.2 s during its passage through the anomaly (Fig. 1*a*), and this delay remains almost unchanged for distances as great as 1,000 km beyond the plume (Fig. 1*b*). At 1,500 km, 80% of the maximum time delay persists. We therefore conclude that there are good prospects for detecting plumes in the lower mantle by seismology.

Here we report the results of our attempt to detect a plume beneath the Bowie hotspot. This case was chosen because of its exceptional geometry: rays from 12 earthquakes from the Alaskan subduction zone, recorded at the 120 stations of the Washington Regional Seismic Network (WRSN), illuminate the postulated plume in a fan-like fashion. We determine relative arrival times by multi-channel cross-correlation, with a precision better than 0.05 s. We then separate the different contributions to the travel-time anomalies, and find a slow region, located ~150 km away from the vertical of Bowie. We suggest that this anomaly is indeed due to the presence of a plume in the lower mantle.

The exceptional detection geometry

We analyse the first-arriving P-waves from earthquakes at intermediate depth in the Alaskan subduction zone, recorded at the WRSN. Figure 2 shows that rays from these earthquakes to the

Permanent address for H.C.N.: Département Terre-Atmosphère-Océan, Ecole Normale Supérieure, 24 rue Lhomond, 75231 Paris 05, France. J.V.D. is also at the Geophysics program AK-50, University of Washington, Seattle, USA.

network should travel very close to the expected position of the Bowie plume, if it exists. The Bowie hotspot is thought to be responsible for the Pratt–Welker (or Kodiak–Bowie) linear chain of seamounts, clearly visible on a topographic map, to the northwest of the Bowie seamount[23,24]. The map is centred on the position of the Bowie seamount.

The advantages of this configuration are as follows. The WRSN is a wide and dense network of more than 120 digital short-period seismographs, which has been in operation for more than 10 years (ref. 25). The network triggers on teleseismic events, and the corresponding seismograms are carefully archived. Intermediate-depth earthquakes are fairly frequent in the Alaskan subduction zone. Because there is both local and regional station coverage, hypocentres are well determined. Rays from these events to WRSN depart from the Alaskan slab almost perpendicular to the strike of the trench, and then travel in a purely oceanic region. The stations are not located too far behind the expected plume, so that we can hope that the small delay we look for is preserved when the waves reach the stations. Finally a detailed study of upper mantle structure beneath the array[26] indicates that rays arriving from the northwest are least affected by the presence of the slab that has subducted beneath the continent there.

There are also some disadvantages, related to the Bowie hotspot itself, and to the geometry of the experiment. Although it has left a clear and typical track of seamounts on the sea floor, the Bowie hotspot is not a 'strong' hotspot (such as Hawaii)[18]. There is no marked topographic swell around the Bowie seamount, and alternative positions have been proposed for this hotspot[27]. As shown in the inset of Fig. 2, the rays that we analyse intersect the hypothetical Bowie plume in the lower mantle, making it impossible to seek the presence of the plume in the upper mantle. The structure beneath WRSN is complex, and strong lateral variations are present, both in the crust and in the upper mantle.

Accurate determination of travel-times

Here we build a profile of travel-time variations as a function of the distance Δ_H from the presumed position of the Bowie hotspot (53.5° N, 135.6° W)[23]. Δ_H is measured as the closest distance between each ray and the vertical of the hotspot. As we expect a signal of the order of a few tenths of a second only, emphasis has been laid on getting very accurate measurements. Only intermediate-depth earthquakes with simple, impulsive waveforms have been used (Table 1). The analysis then proceeds in four steps.

First, for each event (e), relative times $t_x^{e,s}$ are determined, using a multi-channel cross-correlation technique[25]. Figure 3 shows examples of the alignment of the waveforms achieved. We only keep sets of stations (s) yielding an average standard

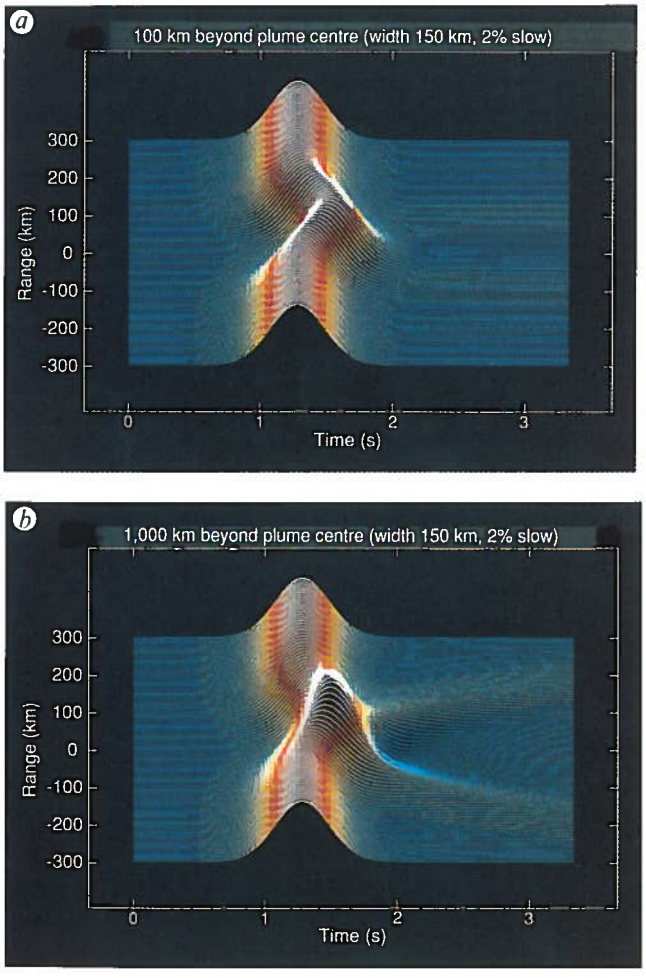

FIG. 1 Synthetic seismograms[22] for a plane wave travelling through a cylindrically symmetric plume. *a*, 100 km; *b*, 1,000 km beyond the centre of the plume.

TABLE 1 USGS hypocentres of the Alaskan earthquakes used here

Date Year/Month/Day	Time hr:min:s	Latitude (°)	Longitude (°)	Depth (km)	m_b ⊥	$\delta_\perp$ (km)	$\delta_\parallel$ (km)
1982/07/14	12:15:47.64	60.514	−153.670	157	5.0	1.4	2.1
1983/04/19	19:12:48.89	63.371	−149.957	112	5.1	0.0	3.8
1983/08/06	16:33:58.36	60.529	−153.129	137	5.4	1.8	−2.5
1983/09/26	23:52:52.91	57.445	−156.395	84	5.4	1.2	−0.6
1984/06/05	01:44:21.48	56.901	−157.262	94	5.3	0.4	−10.3
1987/07/25	01:11:48.86	60.155	−153.771	166	5.0	4.2	−6.1
1988/02/07	08:46:58.61	60.296	−152.972	137	5.6	−4.1	−24.1
1988/11/30	08:55:30.65	61.348	−152.270	143	5.5	−1.2	−26.1
1988/12/22	10:42:12.46	53.983	−166.244	76	5.4	2.9	9.3
1989/03/20	01:06:32.90	59.883	−153.692	127	5.1	−0.4	4.3
1990/05/09	02:38:57.4	57.502	−155.695	77	5.2	−9.7	0.7
1990/08/13	23:04:20.5	60.115	−152.006	88	5.3	NA	NA

$\delta_\perp$ ($\delta_\parallel$) is the mislocation perpendicular (parallel) to the mean azimuth to WRSN, between the ISC hypocentre, and PDE USGS determination, which is the one listed here. The depth mislocation is included in the parallel mislocation. A systematic relocation of events, using ISC arrivals, the IASP91 model, and P, pP, pwP, PKPdf phases was recently done by E. R. Engdahl (personal communication). His results, available for four of our events, yield mislocations that are comparable with the ones reported here, except that the redetermined depths are closer to the PDE depths.

deviation less than 0.05 s. The stack (Fig. 3, top) reveals a simple waveform. At individual stations, the waveform often seems more complicated because in the distance range considered (21° to 26°), two waves arrive within a few seconds; the wave that has its bottoming point below the 660-km discontinuity (Pt660), and the wave that stays above it (Pn660). In the following, we keep only stations for which the Pt660 wave arrives first.

The second step is to calculate theoretical travel-times $t^{c,s}_{theor}$, using the radial model IASP91[28], and a residual time is formed: $t^{c,s}_{res} = t^{c,s}_{x} - t^{c,s}_{theor}$.

We then invert for a smooth single-valued function of residual travel-time against Δ_H. As much of the variation in travel-time residuals can be attributed to lateral heterogeneities in the crust and upper mantle beneath the stations, we perform a simultaneous inversion for the functional values and for station and

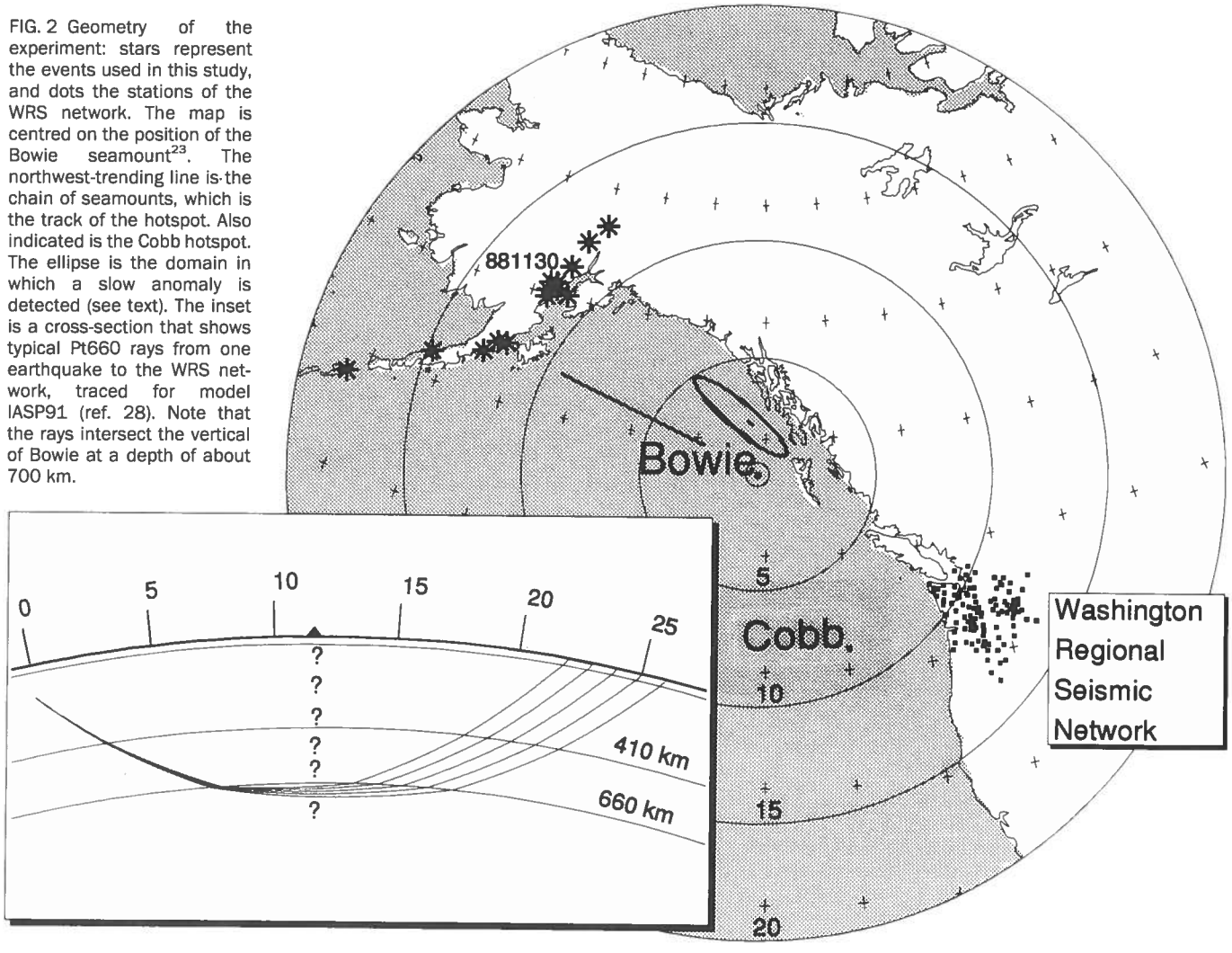

FIG. 2 Geometry of the experiment: stars represent the events used in this study, and dots the stations of the WRS network. The map is centred on the position of the Bowie seamount[23]. The northwest-trending line is the chain of seamounts, which is the track of the hotspot. Also indicated is the Cobb hotspot. The ellipse is the domain in which a slow anomaly is detected (see text). The inset is a cross-section that shows typical Pt660 rays from one earthquake to the WRS network, traced for model IASP91 (ref. 28). Note that the rays intersect the vertical of Bowie at a depth of about 700 km.

event statics t_O^s and t_O^e (because the overall event origin times are also relatively unconstrained). We regularize the inversion by minimizing both the first and second differences of the function. Our inversion method is made robust by iteratively performing least-squares inversions, and down-weighting outliers (defined as data residuals greater than 1.5 standard deviation from the curve) at each iteration[29,30]. The standard deviation is defined at each point on the curve by the residuals in a 1-degree interval assuming that the number of degrees of freedom is represented by the number of data points within each interval minus 1 (ref. 31). This is not strictly correct, as we have reduced the number of degrees of freedom through both the regularization of the problem and the inclusion of station and event statics. The end result of this process is to attribute as much data variance as possible to the static corrections while obtaining a curve with the least amount of structure necessary to explain the remaining travel-time residuals, as obtained from the expression $t_{cor}^{e,s} = t_{res}^{e,s} - t_O^s - t_O^e$.

Finally, corrected relative residuals are plotted as a function of Δ_H, the distance from the ray to the vertical of Bowie.

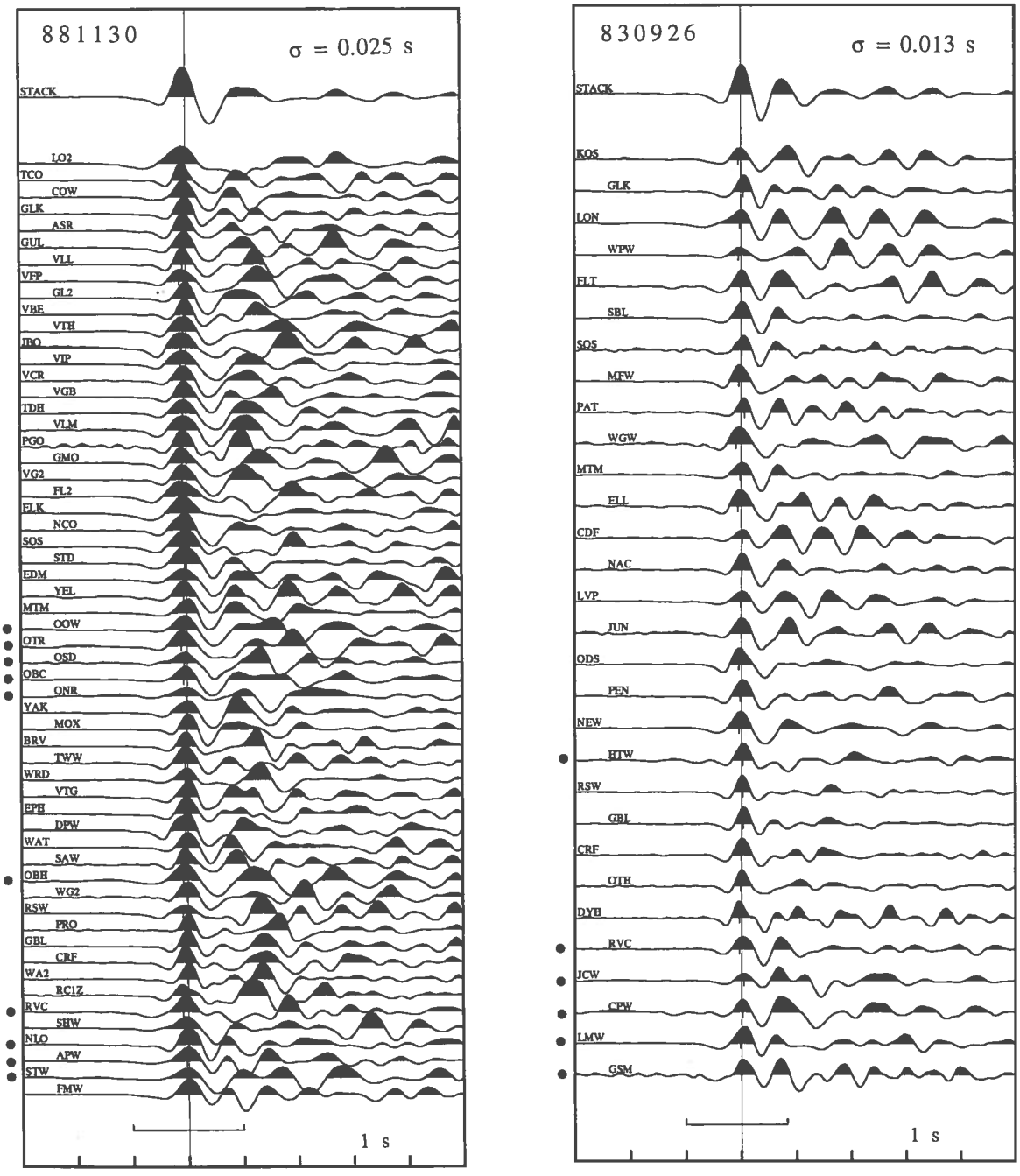

FIG. 3 Seismograms for events 881130 and 830926, as aligned through the multi-channel cross-correlation technique of VanDecar and Crosson[25]. The traces have been low-pass filtered at 5 Hz. The top trace is the stack of the most similar waveforms, and is representative of the source wavelet. The bar at the bottom gives the time window used in the cross-correlation. The vertical tic on each trace is the starting visual pick. The average timing standard deviation σ is indicated. For the stations marked with a dot, the first arrival is Pn660 instead of Pt660 (see text): these records have not been used in the rest of the analysis.

Detection of a mantle plume?

Figure 4*a* shows the plot of $t_{cor}^{e.s.}$ against Δ_H, for the 12 events. The scatter of the data is consistent with our estimated accuracy of about 0.1 s. Also drawn is the continuous curve of residuals against Δ_H as determined in the inversion process. The dashed lines give the standard deviation of the data around that curve. The bar at the bottom gives the size of the quarter-period Fresnel zone (defined as the region through which non-Fermat rays can pass and still arrive within a quarter-period from the Fermat ray) in the transverse direction to Δ_H. Although no clear pattern emerges around the expected plume position ($\Delta_H = 0°$), a clear bell-shaped signal is visible around $\Delta_H = 1.5°$. The delays reach a maximum of about 0.15 s, over a width of ~150 km. A smaller bump also appears around $\Delta_H = -1°$, but this is produced by data from a single earthquake, and we do not think that it is really resolved.

The most straightforward, and exciting, interpretation of our results is that we have detected a plume beneath the Bowie hotspot. In Fig. 4*b*, our smooth function, together with its 90% confidence limits, is superimposed on a plot of the delays predicted from the 'lower bound' and 'upper bound' models previously discussed. We see that the diameter of the anomaly we observe is close to the lower bound estimate, whereas the time-delay is about 1.5 times larger. As our inversion produces a 'minimal curve', the actual time-delay might be somewhat larger, as suggested by the individual trends of some events.

Before going further into the implications of this finding, we should consider the likelihood of alternative explanations of our observations.

Near-source effects. For any given event, rays to WRSN leave the source within an azimuth window of 10°. If the bell-shaped anomaly is caused by a structure in the subducting plate, say 200 km thick, then the structure should be only 20 km wide. This is less than the distance between events 881130 and 880207, which do seem to show a coherent pattern. We could check, by removing one event at a time, that the position of the anomaly was not dependent on a single event. However, the amplitude of the anomaly is mostly constrained by the 881130 event, and to a lesser extent by the 880207 event. On the other hand, the small bump visible for Δ_H around $-1°$ disappears entirely if the 881222 event is not included.

Near-receiver effects. A structure that could explain the bell-shaped delays would have to be present beneath a large part of the array. It should then also be seen for the other events, and in fact enter the 'station static correction'. The structure beneath the array being rather complex, some differential effect could remain, which could explain the observed pattern. To test this effect, we have done simple integrations and three-dimensional ray tracing in the tomographic model derived by VanDecar[26] for the region beneath the WRSN. We found that the computed delays were in good agreement with our 'statics', and that, for the considered azimuths, the differences between events were too small to explain our observations, although they certainly contribute to the scatter around our curve.

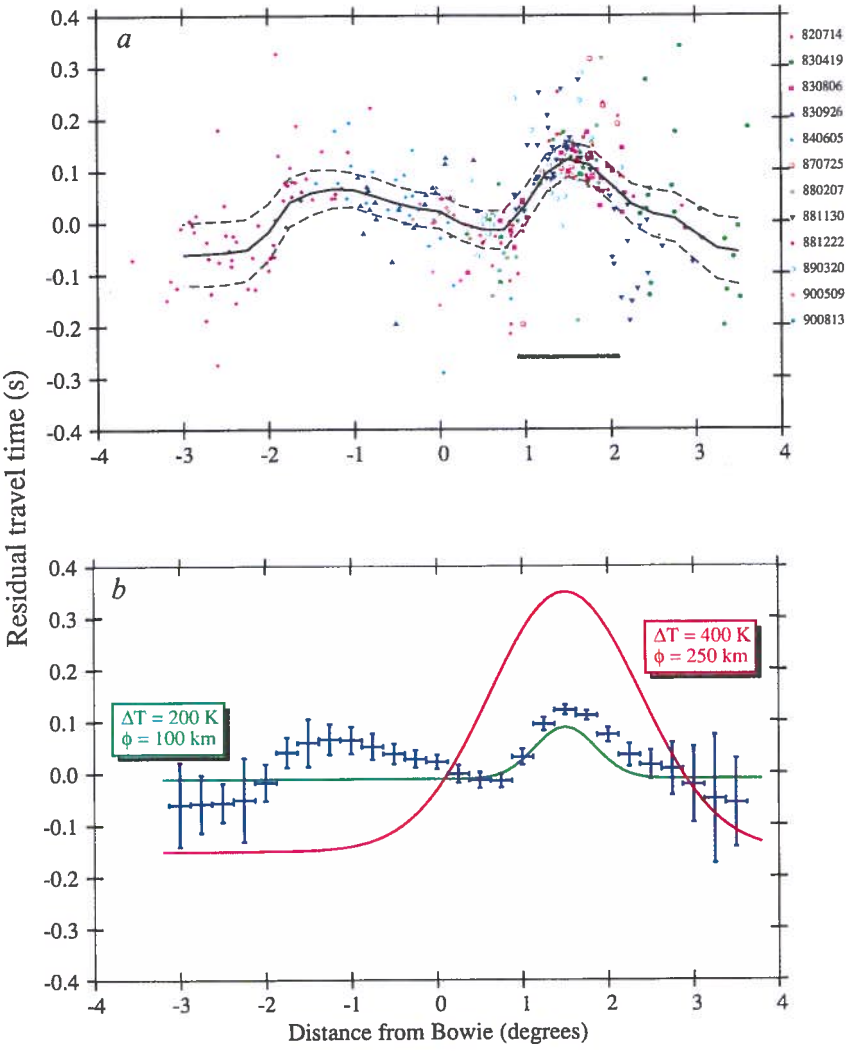

FIG. 4 *a*, Corrected relative residual travel-times as a function of Δ_H, the closest distance of the ray to the vertical of Bowie (counted positive to the northeast). Each plotted earthquake is given a symbol. Note the bell-shaped pattern of events 881130, 830806 and 880207. The solid curve is the best-fit function for residuals against Δ_H, and the dashed curves give the standard deviation of the data (see text). The horizontal bar at the bottom is the size of the quarter-period Fresnel zone. *b*, The best-fit curve shown in *a* (points with error bars) is compared with the expected delay curves for the two plume models discussed in the text (solid lines). The error bars are now the 90% confidence interval for deviations of the mean (see text). All curves have been given a zero mean over the range considered.

Anomalies elsewhere on the path. Our treatment assumes that the anomaly we are looking for is linked to the Bowie hotspot. This is very similar to the approach followed by Creager and Jordan[32] for detecting slab penetration into the lower mantle. Obviously, our path coverage does not allow a full-size tomographic inversion to be done. However, our geometry does give some stereoscopic vision. We tried to evaluate where our 'image' was best in focus by running inversions for different trial positions of the Bowie plume along a line that could give an anomaly at $\Delta_H = 0°$. We found the anomaly was best focused (maximum height ratio of scatter) in the elliptical domain shown in Fig. 2.

Inadequacy of the radial model. We found that model IASP91[28] could predict arrival times remarkably well. As we only deal with relative arrival times, it only matters that the slope and shape of the travel-time curve be accurate. This was apparently the case, as we did not find any correlation of residuals with epicentral distance for the Pt660 branch (most observations) but as the cross-over from Pn660 to Pt660 branch involves a strong change in slope, and is very sensitive to the exact model, distance and depth of the event, the residuals for the Pn660 branch had a scatter of up to 0.2 s, which correlated with epicentral distance, for a given event. All arrivals from the Pn660 branch were therefore excluded from the analysis. We also ran an inversion where Δ_H was replaced by the epicentral distance. We found no structure, down to $\sim$0.05 s, except for the distances corresponding to event 881222. This event is the farthest one, and the relative station residuals might have to be slightly different for this distance.

Event mislocation. Two components should be distinguished: mislocation parallel to the average azimuth from the event to the network (together with depth mislocation), and mislocation perpendicular to the average azimuth. The two components play a very different role in our analysis.

If we were using absolute travel times, the 'parallel' mislocation $\delta_\parallel$ could be dangerous, as it creates a systematic pattern of delays as a function of azimuth, which could mimic our arcuate trend of residues versus Δ_H. But as we only deal with relative travel-times, the effect is in fact small. We have checked that parallel mislocations or depth mislocations of more than 50 km left the bell-shaped pattern of Fig. 4 almost unchanged. Such values largely exceed the plausible mislocations for that region (R. D. van der Hilst, personal communication, see also Table 1).

The effect of the 'perpendicular' mislocation $\delta_\perp$ is that the wavefronts arrive with an angle different from the expected one, thereby producing a linear trend in the plot of Fig. 4, for a given event. The effect could be pronounced, as a perpendicular mislocation of 20 km produces a linear trend of 0.2 s across the array. By considering rays that depart almost perpendicular to the strike of the Alaskan subduction zone, we reduce this effect. It is well known that the component of mislocation parallel to the strike of the slab is much less than the component perpendicular to the slab. Perpendicular mislocations should not exceed a few kilometres.

Inversion artefact. The structure in Fig. 4 could result from trying to fit a smooth curve to randomly scattered points. We checked that this was not the case by running an inversion in which all Δ_H had been randomly permuted, while events and stations were kept unchanged. No structure was visible in the curve obtained, down to a level of about 0.05 s.

Plume characteristics

At this stage, the detection of the plume cannot be considered definitive. However, we believe that our analysis is the best attempt so far, and is the best that can be done with current data and techniques. The most plausible explanation of the bell-shaped signature in Fig. 4 does seem to be that there is a mantle plume (or diapir) beneath Bowie. If true, this observation has several implications. The diameter of the plume is about 150 km. Its core is at least 1.5% slower than the surrounding mantle. This translates into a temperature contrast of at least 300 K, unless velocity is reduced by additional effects (partial melting or anisotropy). As the rays that we analyse intersect the Bowie plume below the 660 km discontinuity, we are led to conclude that the plume originates below that discontinuity, in the lower mantle. Finally, at $\sim$700 km depth, the centre of the plume is 150 km northeast of the position of the Bowie seamount. Age data suggest that the Bowie hotspot is at present $\sim$100 km southeast of the seamount[24]. Our data indicate that it could be even farther away from the Bowie seamount, or else that the plume is not vertical.

Our results could be tested and extended in a number of ways. The numerous seismic stations on the western margin of North America should make it possible to retrieve longer profiles, and investigate how the anomaly evolves with depth. A detailed analysis of amplitudes and waveforms would put bounds on the internal structure of the plume. Our synthetic seismograms suggest that the anomaly to be expected for the Hawaiian plume should remain detectable as far away as North America. □

Received 15 April; accepted 4 June 1993.

1. Morgan, W. J. *Nature* **230,** 42–43 (1971).
2. Wilson, J. T. *Can. J. Phys.* **41,** 863–870 (1963).
3. McKenzie, D. P., Roberts, J. M. & Weiss, N. O. *J. Fluid Mech.* **62,** 465–538 (1974).
4. Anderson, D. L. *Theory of the Earth* (Blackwell, Boston, 1989).
5. Schilling, J. G. *Nature* **352,** 397–403 (1991).
6. Watson, S. & McKenzie, D. P. *J. Petrol.* **32,** 501–537 (1991).
7. Loper, D. E. & Stacey, F. D. *Phys. Earth planet. Int.* **33,** 304–317 (1983).
8. Iyer, H. M. *et al. Geol. Soc. Am. Bull.* **92,** 792–798 (1981).
9. Hadley, D. M., Stewart, G. J. & Ebel, J. E. *Science* **193,** 1237–1329 (1976).
10. Zhang, Y.-S. & Tanimoto, T. *Nature* **355,** 45–49 (1992).
11. Olson, P. & Singer, H. *J. Fluid Mech.* **158,** 511–531 (1985).
12. Kanasewich, E. R. Ellis, R. M., Chapman, C. H. & Gutowski, P. R. *Nature* **239,** 99 (1972).
13. Wright, C. *J. geophys. Res.* **80,** 1915–1919 (1975).
14. Hirahara, K. *J. Phys. Earth* **25,** 393–417 (1977).
15. Humphreys, E., Clayton, R. W. & Hager, B. H. *Geophys. Res. Lett.* **11,** 625–627 (1984).
16. Spakman, W. *Geophys. J. int.* **107,** 309–332 (1991).
17. Davies, G. F. *J. geophys. Res.* **93,** 10467–10480 (1988).
18. Sleep, N. H. *J. geophys. Res.* **95,** 6715–6736 (1990).
19. Kumazawa, M. & Anderson, O. L. *J. geophys. Res.* **74,** 5961–5972 (1969).
20. Peltier, W. R. & Solheim, L. P. *Geophys. Res. Lett.* **19,** 321–324 (1992).
21. Wielandt, E. in *Seismic Tomography* (ed. Nolet, G.) 85–98, (Reidel Dordrecht, 1987).
22. Bostock, M. G., VanDecar, J. C. & Snieder, R. *Bull. seism. Soc. Am.* **83,** 756–779 (1993).
23. Morgan, W. J. *Am. Assoc. Petrol. Geol. Bull,* **56,** 203–213 (1972).
24. Turner, D. L., Jarrard, R. D. & Forbes, R. B. *J. geophys. Res.* **85,** 6547–6556 (1980).
25. VanDecar, J. C. & Crosson, R. S. *Bull. seism. Soc. Am.* **80,** 150–169 (1990).
26. VanDecar, J. C. thesis, Univ. of Washington (1991).
27. Duncan, R. A. & Clague, D. A. in *The Ocean Basins and Margins,* Vol. 7A, *The Pacific Ocean* (eds Naim, A. E. M., Stehi, F. G. & Uyeda, S.) 89–121 (Plenum, New York, 1985).
28. Kennett, B. & Engdahl, E. R. *Geophys. J. Int.* **105,** 429–465 (1991).
29. Egbert, G. D. & Booker, J. R. *Geophys. J. R. astr. Soc.* **87,** 173–194 (1986).
30. Huber, P. J. *Robust Statistics* (Wiley, New York, 1981).
31. Snedecor, G. W. & Cochran, W. G. *Statistical Methods* (Iowa State Univ. Press, Ames, 1967).
32. Creager, K. C. & Jordan, T. H. *J. geophys. Res.* **89,** 3031–3049 (1984).

ACKNOWLEDGEMENTS. We thank L. Fleitout for encouragement, those running the WRS Network (in particular R. Crosson and R. Ludwin) for their work, Bob Engdahl for communicating his relocations of some of our events, W. Spakman, M. DeJong, M. Bostock, M. Remkes, R. Snieder, N. Vlaar and R. Wortel for valuable help, and J. Vidale and E. R. Engdahl for constructive reviews. This research was conducted while H. C. N. was on a sabbatical year in Utrecht, supported by CNRS, INSU, EEC and NATO. J.C.V. was supported by the Netherlands Organizations for Scientific Research, and by the U.S. NSF.